Nanoscale

Accepted Manuscript

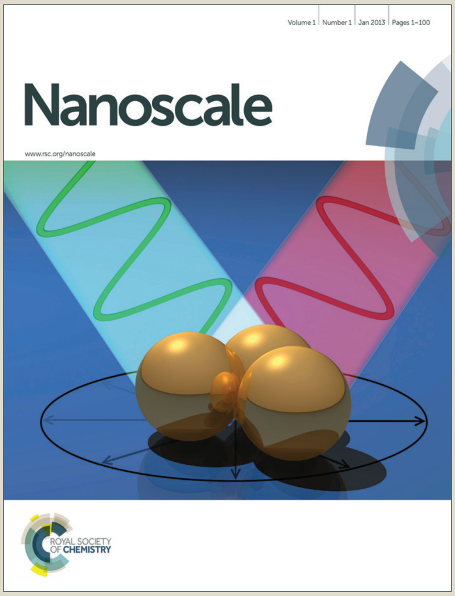

ROYAL SOCIETY OF CHEMISTRY

www.rsc.org/nanoscale

Nanoscale RSCPublishing

COMMUNICATION

Cite this: DOI: 10.1039/x0xx00000x

Formation of Hexagonal boron nitride nanoscrolls induced by Inclusion and Exclusion of Self-assembling molecules in solution process

Received 18th February 2014,
Accepted

DOI: 10.1039/x0xx00000x

www.rsc.org/

Da Young Hwang[a], Dong Hack Suh[*a]

Compared with nanoscroll of 2D graphene, that of 2D h-BN has not been demonstrated except only few experimental reports. Nanoscrolls of h-BN with high yields and reproducibility are first synthesized by a simple solution process. Inner-tube diameter of BNSs included by LCAs, N-(2-aminoethyl)-3α-hydroxy-5β-cholan-24-amide, as a bile acid derivative and self-assembling material can be controlled by adjusting diameter of LCA fiber which is growing by self-assembly. TEM and SEM images show that BNSs have a tube-like morphology and the inner-tube diameter of BNSs is controlled in the range from 20-60nm for a smaller diameter up to 300nm for a larger diameter by LCA fiber growth inside BNSs. Finally, the open cylindrical BNSs with hollow core were obtained by dissolving LCAs inside BNSs.

The two-dimensional (2D) materials[1] such as few-layer crystals of graphene, hexagonal boron nitride (h-BN) and molybdenum disulphide (MoS_2) have attracted great attention in nanotechnology[2]. During the past few years, graphene has been extensively studied in many fields, although smaller than the number on graphene papers, there are a huge number of theoretical and experimental papers on these other 2D crystals, particularly h-BN[3, 4]. h-BN, called white graphene, has electrical insulating[5], superb mechanical properties[6, 7] and high thermal conductivity[8] through the different dimensional types. h-BN can be regarded as the basic 2D building block for other dimensionalities such as 0D nanoball, 1D boron nitride nanotubes (BNNT), 3D bulk h-BN crystals and boron nitride nanoscrolls (BNS), which are new h-BN-based materials and morphologically very similar to graphene nanoscrolls (GNS)[9-12]. Recently, a few researches have been developed for the fabrication of BNSs by shear induced formation[13] and exfoliation of h-BN by molten hydroxides[14]. However, these methods have many disadvantages, including the difficulties about exfoliation of h-BN due to the stronger lip-lip interaction[2] between crystals, expensive equipment and installation costs, etc. Additionally, the scroll mechanism of 2D h-BN crystals has not been explained as well as there has been no report about controlling the inner-tube diameter of BNSs compared with that of BNNT[15, 16].

Here we demonstrate the first and simple synthetic method of Hexagonal Boron nitride scrolls (BNS) using a density gradient method and BNSs made by interaction of the exfoliated h-BN with LCAs as a self-assembling material have a unique structure including LCAs inside BNSs. And the inner-tube diameter of BNSs could be controlled by adjusting diameter size of LCA fiber inside BNSs. We obtain the hollow core BNSs from exclusion of LCAs through both open end points of BNSs dissolved by solvent.

As starting materials, the exfoliated h-BN (<1μm) solution was obtained by a chemical exfoliation method and characterized by Scanning electron microscopy (SEM), Atomic force microscopy (AFM) and Transmission electron microscopy (TEM) (Fig. S1) and synthesis of N-(2-aminoethyl)-3α-hydroxy-5β-cholan-24-amide (LCA) as a bile acid derivative and self-assembling material was reported in supplementary information.
In general, LCAs from the nature amphiphilic molecules have stronger binding affinities for the 2D materials such as graphene[17] and h-BN sheets by noncovalent interaction and can be self-assembly. Also, an amine-functional group of LCAs can strongly interact with h-BN sheets as Lewis acid and base, particularly focusing on its free edge sites[18]. Different from LCAs with three functions of amphiphilicity, self-assembly and Lewis base, other bile acid derivatives such as cholic acid, deoxycholic acid, lithocholic acid, methyl lithocholate and N-(2-aminoethyl)-3α-hydroxy-5β-cholan-24-amide with only one or two functions have been investigated about effective interaction with h-BN sheets. However, BNSs can not be obtained from these materials under the same condition of LCAs fiber growth. It is believed from these results that LCAs strongly interact with h-BN sheets as an important factor in scrolling formation of BNSs.

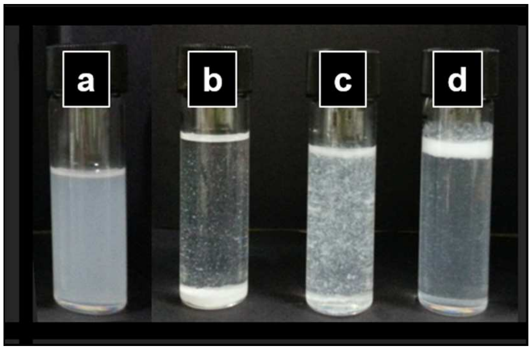

Figure 1. Effect of separation by density gradients of floating precipitates on adding different amounts of LCAs into the exfoliated h-BN solution; Images of (a) the exfoliated h-BN solution of ODCB (5mL) and floating precipitates from (b) 0.01 (c) 0.02 and (d) 0.1mmol of LCAs dissolved in ODCB (1mL).

Using these specific functions of LCAs, hexagonal boron nitride nanoscrolls (BNS) were synthesized by adding the amount of LCAs into the exfoliated h-BN sheets. An amount of LCA in the range from 0.01 to 0.1mmol was dissolved in ODCB (1mL) and heated to 60°C. Then, the dissolved hot solution was immediately poured into the exfoliated h-BN solution of ODCB (5mL) at room temperature. As increasing the amount of LCA adding into the exfoliated h-BN solution, that of the floating precipitates increases by density gradients (Fig. 1). The floating precipitates have almost BNSs while the precipitates of the bottom layer have the mixtures of the aggregated h-BN and multilayers of h-BN, as shown in Fig S2. The density gradients are due to the mass ratio of two components in complexes produced by interaction between the amount of LCA and h-BN sheets in which the density of the h-BN sheets is almost equal to that of ODCB (1.30g/mL) and bigger than that of LCA (1.08g/mL). As a result, as the amount of LCA increases, interaction between h-BN sheets and LCAs increases and the density of the floating precipitates decreases and then the phase separation is induced. Simultaneously, the crude BNSs (C-BNS) were obtained by the floating precipitates due to the decrement of the surface interaction between h-BN sheets and ODCB and of the surface areas of BNSs compared with that of h-BN sheets.

To purify the produced C-BNSs, the solution of the resulting precipitates was stored at room temperature for 24 hrs in order to ensure the phase separation by a larger differences in the density of boron nitride-LCA complex caused by the interaction between h-BN sheets and LCAs in ODCB. And then, the precipitates were obtained by filtering with a PTFE membrane, affording BNSs.

Fig. 2 depict the tube-like morphology srolled by interaction of h-BN sheets with LCAs. Fig. 2a shows the BNSs were produced with high yields and the inner diameter of 20-60nm after adding LCAs of 0.02mmol into the exfoliated h-BN in ODCB. High resolution-TEM (HR-TEM) images (Fig. 2b) indicate the 0.33nm d-spacing in the walls of BNSs, which corresponds to the layer-by-layer distance of h-BN sheets and BNNTs. Likewise, the single BNSs completely rolled up through the cylindrical axis are represented in Fig. 2c-d. As shown in HR-TEM (Fig. 2e-f), the tube end points of BNSs are circular, which is different from those of graphene scrolls (GNS). Previous papers[9, 10] reported that the dispersed graphene prepared by ultrasonication has irregular morphology and defects. But, in our case, the exfoliated h-BN prepared by a homogenized magnetic stirrer without ultrasonication has the originally intact circular shape with no defects. Hence, we suggest that BNSs rolled up from the exfoliated h-BN sheets are regular in shape and have no defects to compare with GNSs. Moreover, BNSs were detected by the elementary analysis of Energy dispersive spectrometer (EDS) images, which confirms the unique structure of LCA-included Boron nitride nanoscrolls (Fig. S3).

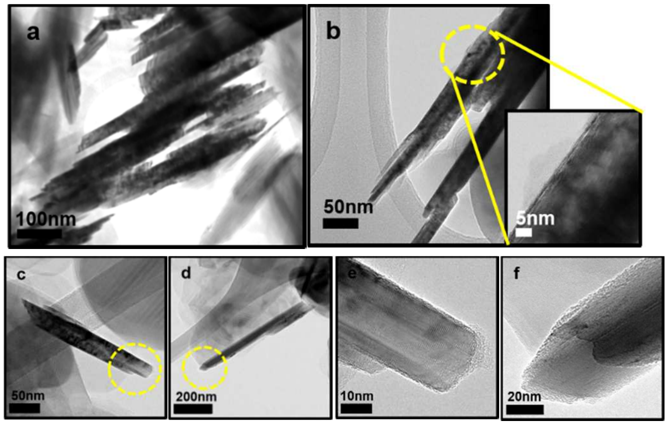

Figure 2. Hexagonal Boron nitride nanoscroll produced from LCAs and the exfoliated boron nitride sheets. (a) TEM images of BNSs with high yield and (b) with 0.33nm d-spacing by magnification. (c-d) HR-TEM images of single BNS rolled up completely and (e-f) with the end points of each edge in (c-d).

We now consider the information of electronic structure and phonon dispersion of the h-BN based materials. Raman spectra of the exfoliated hexagonal boron nitride (<1μm) and Boron nitride nanoscrolls (BNS) are revealed in Fig.3. At first, Raman spectrum of the exfoliated h-BN represents the Full width at half-maximum (FWHM) of 16cm^{-1} at E_{2g} phonon mode (~1364cm^{-1}), which is due to B-N bond vibration and phonon dispersion within a plane[19]. Second, in the case of those of BNSs, the remarkable changes of FWHM of 19cm^{-1} at E_{2g} phonon mode (~1366cm^{-1}) are observed, which shows the blue shift of up to 2cm^{-1} and broadness of up to 3cm^{-1} compared with the exfoliated h-BN. In addition, at E_{2g} mode, it is noticed that the degree of Raman shift and intensity for BNSs are larger than those for the exfoliated h-BN. The blue shift of E_{2g} phonon mode indicated a slightly shorter B-N bond, caused by the isolated monolayers[20] or compressive stresses compared with h-BN sheets and BNNTs[21, 22]. The reason about the blue shift of BNSs at E_{2g} phonon mode is same in our case. Therefore, it is believed that the blue shift and broadness of FWHM give strong evidence to BNSs due to the lip-lip interaction between scrolled h-BN sheets and morphological differences of BNSs.

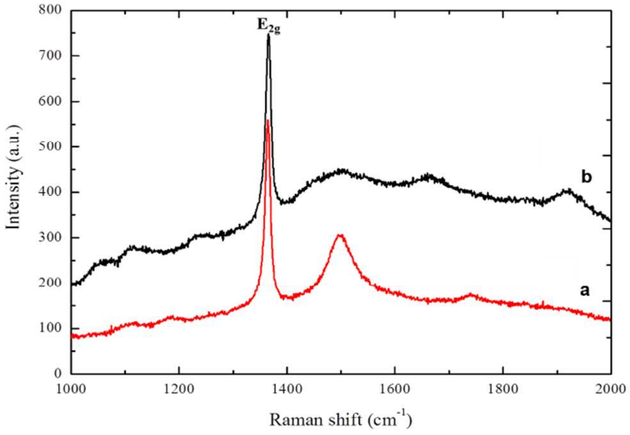

Figure 3. Raman spectra of the exfoliated h-BN and BNSs with laser excitation at 532nm of wavelength. Raman spectra of (a) the exfoliated h-BN and (b) BNSs at E2g phonon mode.

Solid core BNSs, filled with LCA molecules, were classified by two kinds of smaller and larger inner-diameter sizes of BNSs (S-BNSs and L-BNSs, respectively). First, for preparation of solid core S-BNSs, LCA of 0.02mmol was dissolved in ODCB (1mL) and heated to 60°C. Then, the dissolved hot solution was immediately poured into the exfoliated h-BN solution (5mL) at RT. The fiber growth of LCAs themselves is relatively slow due to the increment of the interaction between h-BN sheets and LCAs. And to remove an amount of LCAs more than that of h-BN sheets through dissolution by solvent, C-BNSs were washed with methanol followed by centrifugation at 4000 rpm for 20 minutes and by decantation. This procedure was at least repeated five times. And the solid core S-BNSs were obtained.

Second, for preparation of solid core L-BNSs, LCA of 0.003mmol was dissolved in ODCB (1mL) and heated to 60°C. Then, the dissolved hot solution was stored at room temperature for 24hrs, which create favorable conditions for growing to LCA fiber. In general, it has been known that LCAs grow to fiber in various solvents[23] by intermolecular interaction of hydrogen bonding, hydrophobic interaction and van der Waals forces (Fig. S4). And then LCA fiber solution was poured into the exfoliated h-BN solution at RT and the precipitates were obtained by filtering with a PTFE membrane, followed by centrifugation at 4000 rpm for 20 minutes and by decantation. Here, the LCA fiber as a template interacts with h-BN sheets. As the diameter of the LCA fiber increases, the larger solid core L-BNSs were obtained.

TEM image (Fig. 4a) represents the solid core S-BNSs of few nanometers with the self-assembled LCAs. And a SEM image (Fig. 4b) describes the solid core L-BNSs of 300nm, 900nm length and few micro lengths of LCAs placed on SiO_2/Si substrates. Inner-tube diameter of solid core L-BNSs compared with that of S-BNSs is larger, which are synthesized by providing a favorable condition for the fiber growth of LCA before adding the LCA solution into the exfoliated h-BN solution. Because the LCAs are recrystallized by cooling the temperature down and grown to fiber on SiO_2/Si substrates, the SEM image shows the grown fiber of LCA inside L-BNSs. Consequently, the inner-tube diameter of BNSs can be controlled by the growth condition of LCA fiber diameter.

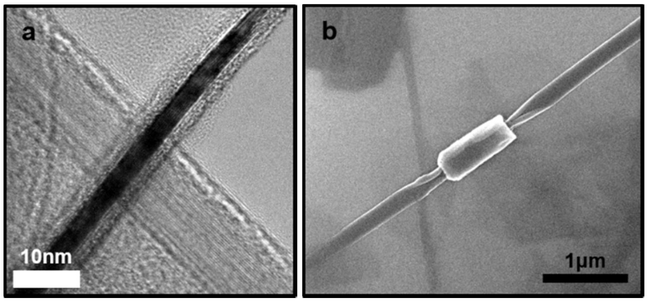

Figure 4. Hexagonal Boron nitide nanoscroll with LCA inclusion and fiber growth. (a) HR-TEM image of BNS tube axis with LCA inclusion. (b) SEM image of BNS with a LCA fiber on SiO2/Si substrates.

Recently, the inclusion of molecules such as water,[24, 25] cations and anions[26] by permeation inside BNNT with a large inner-tube diameter have drawn much attention to the promise applications.[27] However, the experimental difficulties in preparation of BNNTs filled with the desired materials have prevented the development of materials, which is not easy to open the endcaps of BNNTs and remove the encapsulated molecules after the synthesis. Due to the impermeability of h-BN sheets, the solvents cannot penetrate the vertical axis of BNSs. Instead, only the open BNSs at both end points can be permeated through the horizontal axis of BNSs by solvents.

To remove the included LCAs inside BNSs, the obtained S-BNSs were washed with methanol several times in order to have long time enough to dissolve LCAs due to the impermeability through the vertical axis of BNSs. Here, the TEM image describes the partially dissolved LCAs inside S-BNSs (Fig. 5a). Furthermore, after dissolving LCAs with methanol for few days, LCAs inside S-BNSs were completely removed resulting in only hollow core S-BNSs of 25nm inner diameter (Fig. 5b).

The SEM images (Fig. 5c-d) also represent hollow core L-BNSs after washing LCA with the methanol, and L-BNSs with large hollow core of 125nm inner diameter through SEM at tilt angle of 60°. From the procedure, BNSs can be easily included by LCA and excluded through the both open end points of BNSs dissolved by solvent and degraded by heat.

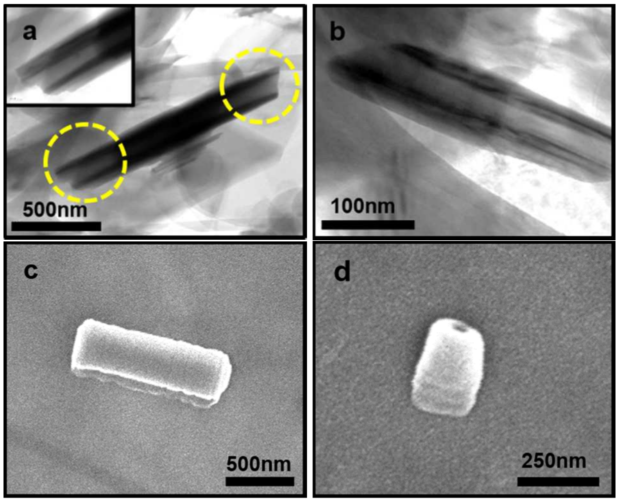

Figure 5. Removal of self-assembled LCAs inside Hexagonal boron nitride nanoscrolls by methanol. (a) TEM images of S-BNSs with partial dissolution of LCAs inclusion at the both end points and (b) the hollow core BNSs with the complete dissolution of LCAs. (c) SEM images of BNSs after washing LCA with the methanol and (d) with the hollow core at tilt angle 60°.

Formation mechanism of Boron nitride nanoscrolls induced by LCA

The TEM images (Fig. 6) depict the formation of BNSs, which is involved in (a) prinstine h-BN sheets, (b-c) the initial state of h-BN scrolling gradually after adding LCAs of 0.02mmol into the exfoliated h-BN solution and (d) the end state of full h-BN scrolling.

The interaction of h-BN with the amine-functional group of LCAs is very important for understanding formation mechanism of Boron nitride-LCA nanoscolls. In the energy aspect of interaction, the amine-functional group of the LCA fiber has the interaction on the entire sheets of h-BN but strong interaction on the edge of the more unstable part because the edge of h-BN have the lowest energy of bond length, angles, dipole moments and adiabatic adsorption, particularly, at the edge of h-BN sheets[18]. Therefore, scrolling occurs at the edge of h-BN sheets.

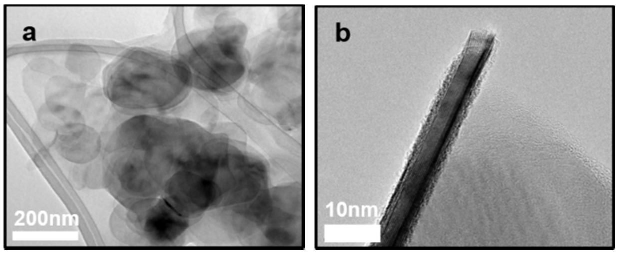

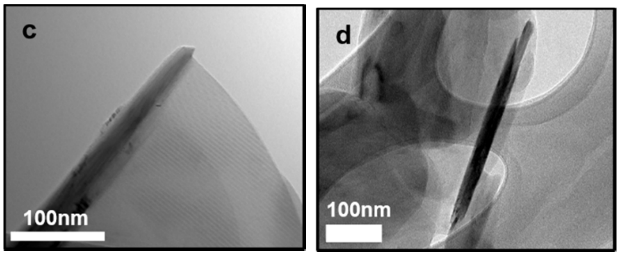

Figure 6. Formation of Hexagonal boron nitride nanoscrolls from the edge of the h-BN sheets. TEM images of (a) pris-tine hexagonal boron nitride, (b-c) the initial state of h-BN scrolling and (d) the end state of h-BN scrolling.

For the formation of scroll, similar to GNSs,[28] three driving forces are needed for BNSs; One is the interaction of h-BN with the amine-functional group of LCAs as Lewis acid and base, which effect the scrolling of h-BN sheets spontaniously (increasing stability). Another is bending of the h-BN sheets (decreasing stability) and the other is rolling h-BN with van der Waals interaction energy of π-π overlapping (increasing stability).[3] Using these driving forces, the interaction energy between h-BN sheets and the amine-functional group of LCAs is defined as[29, 30]

$$E_{\text{interaction}} = E_{\text{total}} - (E_{\text{boron nitride}} + E_{\text{LCA}})$$

where E_{total} is the total potential energy of BNSs formation and $E_{\text{boron nitride}}$ and E_{LCA} are the energy of the each prinstine structure. As soon as adding the amount of LCAs into the exfoliated h-BN solution, although the two sides of h-BN sheets have the same opportunities, one side of h-BN sheets slightly more interacted with the amine-functional group of LCAs by subtle differences in the interaction. As this interaction gradually increases, rising and bending of h-BN sheets at the edge occur. Simultaneously, $E_{\text{interaction}}$ increases by the decrement of lip-lip interaction between neighboring h-BN sheets. However, the interaction of h-BN sheets with the amine-functional group of LCAs has a counterbalance energy to the sp^2 hybridization interaction. At the same time, as LCAs gradually grow to fiber by self-assembly, the h-BN sheets have a first cycle rolling up by the interaction energy enough to overcome the energy of h-BN sheets. The inner diameter of BNSs is bigger than that of GNSs due to the small 20-100MPa elastic modulus of h-BN sheets[31] compared with 1Tpa of graphene[32], which results in the loose π- π interaction. As srolling process is initiated, $E_{\text{boron nitride}}$ gradually increases because of the bond bending, stretching and the decrement of overlapping graphene π- π interaction. and E_{LCA} is fixed as a scrolling template after rolling up to a first cycle. After a first cycle scrolling, h-BN rolling with π-π interaction increases the stability.

Accordingly, the total potential energy of BNSs formation is due to differences of interaction energy between LCAs and h-BN sheets and energy of pristine h-BN heets. The inner-tube diameter of BNSs depends on the surface area of the exfoliated h-BN sheets and the diameter of LCA template where the scrolling process occurs.

In summary, Hexagonal boron nitride nanoscrolls with high yields were first synthesized by a simple solution process and separated by a density gradient method. The inside of the resulting BNSs is included by LCAs as a self-assembing molecule, which is able to control the inner-tube diameter of

BNSs by diameter of LCA fiber and also can be excluded inside BNSs by solvent. The TEM images show that S-BNSs have a tube-like morphology with inclusion of LCAs. The SEM images show the open cylindrical structure of L-BNSs included by the fiber growth of LCA by self-assembly, which is caused by adding LCA fiber into the exfoliated h-BN solution, resulting in L-BNSs. Raman spectroscopy confirms that the blue shift and broadness of FWHM give strong evidence to the electronic structure of BNSs. In addition, the TEM and SEM images show the dissolution of LCAs from both end points to center of the hollow core S-BNSs of 25nm and L-BNSs of 125nm inner diameter.

In conclusion, a new way was developed to insert and draw out the desired material into the inside of hexagonal boron nitride nanoscrolls and also their inner-tube diameter can be controlled by adjusting the diameter of LCA fiber. By carefully selecting the Lewis base and the reaction conditions, the approach might be potentially useful for the preparation of complex of hexagonal boron nitride nanoscrolls and desired materials. The final goal of these efforts is the detailed evaluation of their advanced properties required for future high-performance composites, nano-, bio-, electromechanical, and medical devices.

This research was supported by Basic Science Research Program through the National Research Foundation of Korea (NRF) funded by the Ministry of Education, Science and Technology (2011-0006268)

Notes and references

[a] Division of Chemical Engineering, College of Engineering, Hanyang University, Seoul, 133-791, Republic of Korea

† Electronic Supplementary Information (ESI) available: [details of any supplementary information available should be included here]. See DOI: 10.1039/c000000x/

1 J. N. Coleman, M. Lotya, A. O'Neill, S. D. Bergin, P. J. King, U. Khan, K. Young, A. Gaucher, S. De, R. J. Smith, I. V. Shvets, S. K. Arora, G. Stanton, H. Y. Kim, K. Lee, G. T. Kim, G. S. Duesberg, T. Hallam, J. J. Boland, J. J. Wang, J. F. Donegan, J. C. Grunlan, G. Moriarty, A. Shmeliov, R. J. Nicholls, J. M. Perkins, E. M. Grieveson, K. Theuwissen, D. W. McComb, P. D. Nellist and V. Nicolosi, Science, 2011, 331, 568-571.

2. A. K. Geim and I. V. Grigorieva, Nature, 2013, 499, 419-425.

3. E. Perim and D. S. Galvao, Nanotechnology, 2009, 20, 335702.

4. E. Perim, R. Paupitz and D. S. Galvão, Journal of Applied Physics, 2013, 113, 054306.

5. K. Watanabe, T. Taniguchi and H. Kanda, Nat Mater, 2004, 3, 404-409.

6. E. Hernández, C. Goze, P. Bernier and A. Rubio, Physical Review Letters, 1998, 80, 4502-4505.

7. D. Golberg, P. M. F. J. Costa, O. Lourie, M. Mitome, X. Bai, K. Kurashima, C. Zhi, C. Tang and Y. Bando, Nano Letters, 2007, 7, 2146-2151.

8. C. Zhi, Y. Bando, C. Tang, H. Kuwahara and D. Golberg, Advanced Materials, 2009, 21, 2889-2893.

9. L. M. Viculis, J. J. Mack and R. B. Kaner, Science, 2003, 299, 1361.

10. M. V. Savoskin, V. N. Mochalin, A. P. Yaroshenko, N. I. Lazareva, T. E. Konstantinova, I. V. Barsukov and I. G. Prokofiev, Carbon, 2007, 45, 2797-2800.

11. J. Zheng, H. Liu, B. Wu, Y. Guo, T. Wu, G. Yu, Y. Liu and D. Zhu, Adv Mater, 2011, 23, 2460-2463.

12. T. Sharifi, E. Gracia-Espino, H. Reza Barzegar, X. Jia, F. Nitze, G. Hu, P. Nordblad, C. W. Tai and T. Wagberg, Nature communications, 2013, 4, 2319.

13. X. Chen, R. A. Boulos, J. F. Dobson and C. L. Raston, Nanoscale, 2013, 5, 498-502.

14. X. Li, X. Hao, M. Zhao, Y. Wu, J. Yang, Y. Tian and G. Qian, Adv Mater, 2013, 25, 2200-2204.

15. R. Arenal, O. Stéphan, M. Kociak, D. Taverna, A. Loiseau and C. Colliex, Physical Review Letters, 2005, 95, 127601.

16. R. Ma, Y. Bando, T. Sato and K. Kurashima, Chemical Physics Letters, 2001, 350, 434-440.

17. S. Radic, N. K. Geitner, R. Podila, A. Käkinen, P. Chen, P. C. Ke and F. Ding, Sci. Rep., 2013, 3.

18. E. Anota, A. Juárez, M. Castro and H. Cocoletzi, Journal of molecular modeling, 2013, 19, 321-328.

19. A. Pakdel, Y. Bando and D. Golberg, Chemical Society Reviews, 2014, DOI: 10.1039/C3CS60260E.

20. R. V. Gorbachev, I. Riaz, R. R. Nair, R. Jalil, L. Britnell, B. D. Belle, E. W. Hill, K. S. Novoselov, K. Watanabe, T. Taniguchi, A. K. Geim and P. Blake, Small, 2011, 7, 465-468.

21. T. Kuzuba, Y. Sato, S. Yamaoka and K. Era, Physical Review B, 1978, 18, 4440-4443.

22. R. Arenal, A. C. Ferrari, S. Reich, L. Wirtz, J. Y. Mevellec, S. Lefrant, A. Rubio and A. Loiseau, Nano Letters, 2006, 6, 1812-1816.

23. M. Lofman, J. Koivukorpi, V. Noponen, H. Salo and E. Sievanen, Journal of colloid and interface science, 2011, 360, 633-644.

24. C. Y. Won and N. R. Aluru, Journal of the American Chemical Society, 2007, 129, 2748-2749.

25. T. A. Hilder, D. Gordon and S.-H. Chung, Small, 2009, 5, 2183-2190.

26. T. A. Hilder, D. Gordon and S.-H. Chung, Small, 2009, 5, 2870-2875.

27. W. He, Z. Li, J. Yang and J. G. Hou, The Journal of chemical physics, 2008, 129, 024710.

28. S. F. Braga, V. R. Coluci, S. B. Legoas, R. Giro, D. S. Galvão and R. H. Baughman, Nano Letters, 2004, 4, 881-884.

29. M. Al-Haik, M. Y. Hussaini and H. Garmestani, Journal of Applied Physics, 2005, 97.

30. D. Xia, Q. Xue, J. Xie, H. Chen, C. Lv, F. Besenbacher and M. Dong, Small, 2010, 6, 2010-2019.

31. L. Song, L. Ci, H. Lu, P. B. Sorokin, C. Jin, J. Ni, A. G. Kvashnin, D. G. Kvashnin, J. Lou, B. I. Yakobson and P. M. Ajayan, Nano Letters, 2010, 10, 3209-3215.

32. C. Lee, X. Wei, J. W. Kysar and J. Hone, Science, 2008, 321, 385-388.

33. A. Valkonen, M. Lahtinen, E. Virtanen, S. Kaikkonen and E. Kolehmainen, Biosensors and Bioelectronics, 2004, 20, 1233-1241.

A graphical abstract for the **Table of contents**